Progress In Electromagnetics Research M, Vol. 17, 237–251, 2011

PARTICLE SWARM OPTIMIZATION OF ANTENNA ARRAYS WITH EFFICIENCY CONSTRAINTS

K. A. Papadopoulos, C. A. Papagianni, P. K. Gkonis I. S. Venieris and D. I. Kaklamani

School of Electrical and Computer Engineering
National Technical University of Athens
9, Iroon Polytechneioy Str., 15773, Zografou, Athens, Greece

Abstract—Phased array antennas are a viable solution to a number of problems related to radio communications applications. In this work, the multi-objective stochastic MOPSO algorithm is used to optimize the spatial configuration of a symmetric phased linear array. The defined optimization goals were the suppression of the radiation pattern sidelobes at a specified maximum scan angle as well as the minimization of the induced voltages correlation at the receiver front-end in order to maximize diversity performance. Non-linear constraints were enforced on the solution set, related to the multi-antenna system aperture efficiency and related to the mismatching when the array is scanned. The obtained optimized configurations for an array composed of 16 dipoles resulted in reducing the sidelobes up to 2.5 dB, when scanned 60° away from broadside, compared to a linear array with elements spaced $\lambda/2$ apart. Furthermore, the optimized dipole arrays were characterized by a maximum element correlation of 0.12 to 0.43. The performance of obtained configurations was shown to be tolerant to feed phase variations that appear in realistic implementations. The arrays were analyzed employing the Method of Moments (MoM).

1. INTRODUCTION

One of the problems that antenna engineers face is the design of prototype antennas which can simultaneously meet the radiation and integration requirements, of the telecommunication system under development. When multiple radiators are incorporated in the antenna system to achieve versatile beam forming capabilities and high diversity

Received 25 January 2011, Accepted 25 March 2011, Scheduled 30 March 2011
Corresponding author: Konstantinos A. Papadopoulos (kpapadop@esd.ece.ntua.gr).

performance, additional constraints rise regarding the implementation of the feeding network and receiver front-end.

The use of modern optimization techniques has helped substantially in the management of escalated complexity that is inherent in the design and integration process. Particle Swarm Optimization (PSO) is a nature inspired algorithm that mimics the behavior patterns of a swarm of bees in search of food [1]. PSO has been reported to successfully obtain optimal parameter values for a number of antenna design and array synthesis problems, such as phased arrays pattern synthesis, adaptive tuning of phased array coefficients to minimize interferences, conformal antenna array amplitude tapering and patch antennas [2–5]. The PSO algorithm was extended to allow the optimization of multiple objectives (MOPSO), without resorting to a weighted aggregation scheme for the corresponding fitness values [6]. The MOPSO algorithm has been applied to antenna design problems specifying the fulfillment of partially contradicting objectives, such as narrow beamwidth versus highly suppressed sidelobes for the radiation pattern of linear arrays [7], or return loss and fidelity factor of ultra-wideband monopoles [8].

A number of studies have highlighted the effects of mismatching during the scanning of a phased array and how it can be alleviated by placing restrictions on the driving-point impedance of each radiator [9], or have determined conditions under which mutual coupling can be used to improve array gain [10]. Another important effect of mutual coupling is on the diversity performance of arrays; Wallace and Jensen have developed a rigorous network analysis method for determining the correlation of closely spaced antennas [11], while Broydé and Clavelier have proposed a methodology for designing receiver front-ends that take advantage of coupling to improve diversity performance [12].

In this work we describe a methodology for optimizing the spatial configuration of a symmetrical linear dipole array with low voltage correlation among the receiver branches, while at the same time the radiation pattern sidelobes are suppressed at a specified maximum scan angle. The array is conjugate matched to the source network for broadside radiation and constraints are placed on the maximum mismatch during scanning. The MOPSO algorithm is used to optimize candidate configurations; the obtained results indicate that there is a limit to how closely the uniformly excited radiators can be placed to suppress sidelobes, without resulting to high array correlation values. To the best of the authors' knowledge, this is the first study that combines goals related to the radiation and diversity performance of arrays, taking also under consideration the receiver front-end.

The paper is organized as follows. Section 2 presents the formulation used to compute the radiation of a dipole array based on

the Hallen integral equations, the aperture and matching efficiencies and the voltages correlation at the receiver front-end. In Section 3, the optimization goals on sidelobe suppression and correlation minimization, along with the accompanying constraints are laid out in detail. In Section 4, the performance of the resulted configurations is compared to uniform linear arrays with comparable apertures. Finally, the corresponding patterns' sidelobes sensitivity to feed phase variations is determined, and a performance envelop is established.

2. FORMULATION

2.1. Dipole Array

Let us assume that the z-axis oriented dipole radiators constituting an antenna array are center-fed by voltage generators V_i and the respective currents distributions induced by the generators and the radiators' mutual interaction are denoted as $I_i(z)$, where i is the radiator index. In this case, the Hallen-Pocklington integral equations can be used to relate the electric fields E_z to the vector potentials V_{ij} [13].

A formulation that allows the numerical solution of the derived system of integral equations is described by Orfanidis [14]. Specifically, the discretized Hallen system of equations may be written as

$$\sum_{j=1}^{K} \sum_{m=-M}^{M} Z_{ij}(n,m) I_j(m) = C_i \cos(kz_n) + V_i \sin(k\,|z_n|) \qquad (1)$$

where Z_{ij} are impedance values obtained using the approximate Green's function kernel for $i \neq j$ and the exact kernel for $i = j$ with the latter being dependent on the wire diameter a, C_i are constants determined by enforcing the current to be zero at the dipoles ends, and $z_m = m\Delta_j$ is the discretization of each radiator into $2M + 1$ wire segments. For evaluating (1), the symmetrical around $z = 0$ current distributions are approximated using triangular basis functions.

The mutual coupling matrix $\mathbf{Z_{tt}}$ is comprised of self $Z_{ij|i=j}$ and mutual $Z_{ij|i\neq j}$ impedances, evaluated by reducing the discretized Hallen system of equations for the element i and for the elements i and j respectively, and solving for unitary excitation at port i.

2.2. Feeding Network and Matching

If the antenna array is viewed as a multi-port microwave network, then the reflected voltage waves $\mathbf{b_t}$ at the input ports can be computed from the incident waves $\mathbf{a_t}$ by means of the $\mathbf{b_t} = \mathbf{S_{tt}}\mathbf{a_t}$ relation. The

S-parameters can be evaluated from the array impedance matrix $\mathbf{Z_{tt}}$, when a reference system impedance value Z_0 is specified [15], using

$$\mathbf{S_{tt}} = (\mathbf{Z_{tt}} - \mathbf{Z_0^{\dagger}})(\mathbf{Z_{tt}} + \mathbf{Z_0})^{-1} \tag{2}$$

where $\mathbf{Z_0}$ is a diagonal matrix with its elements equal to the reference impedance and the symbol † denotes a hermitian matrix.

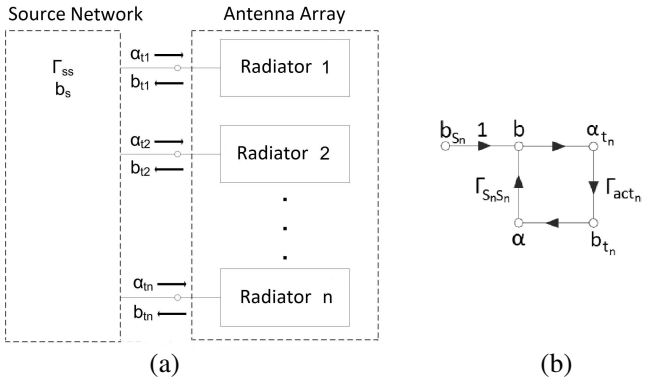

Figure 1. (a) Source network and antenna array as a microwave network. (b) Signal flow graph of Thevenin equivalent circuits.

The source network in Fig. 1 is represented by the $\mathbf{\Gamma_{ss}}$ matrix, which generally is non-diagonal for coupled feeds. Source voltage waves $\mathbf{b_s}$ can be related to voltage waves $\mathbf{a_t}$ using signal flow graphs [16].

$$\mathbf{a_t} = \mathbf{\Gamma_{ss}}\mathbf{b_t} + \mathbf{b_s} = (\mathbf{I} - \mathbf{\Gamma_{ss}}\mathbf{S_{tt}})^{-1}\mathbf{b_s} \tag{3}$$

The derived network formulation is general enough to allow the description of a corporate feed network, a series feed network or individual transmitters for a phased array. For the purposes of this study the latter is assumed and consequently $\mathbf{\Gamma_{ss}}$ is a diagonal matrix.

Maximization of the transferred power to the array, regardless of the applied excitations, requires the implementation of a hermitian matching network which is complex to realize with realistic components, as indicated in the study by Weber et al. [17]. Alternatively, the active reflections at the array ports, computed as the ratio of the incident to the reflected voltage waves, can be conjugately matched; then the main diagonal values of $\mathbf{\Gamma_{ss}}$ equal $\mathbf{\Gamma^*_{act,i}}$.

The total array input power P_{in} can be computed as the power incident to the array ports minus the reflected power. Namely,

$$P_{in} = \mathbf{a_t^{\dagger}}\mathbf{a} - \mathbf{b_t^{\dagger}}\mathbf{b} = \mathbf{a_t^{\dagger}}(\mathbf{I} - \mathbf{S_{tt}}\mathbf{S_{tt}^{\dagger}})\mathbf{a_t} \tag{4}$$

The available power P_{av} is the power that would be delivered to the antenna, if it was hermitian matched to the feeding network. Using (3) it is shown that

$$P_{av} = \mathbf{b_s^\dagger b_s} = \mathbf{b_t^\dagger}\left[\mathbf{I} - \mathbf{\Gamma_{ss}\Gamma_{ss}^\dagger}\right]^{-\mathbf{1}}\mathbf{b_t} \tag{5}$$

A matching factor q can be defined as the ratio of power delivered to the array to available power from the source network [15], as follows

$$q = \frac{P_{in}}{P_{av}} = \frac{\mathbf{a_t^\dagger}(\mathbf{I} - \mathbf{S_{tt}S_{tt}^\dagger})\mathbf{a_t}}{\mathbf{b_t^\dagger}\left[\mathbf{I} - \mathbf{\Gamma_{ss}\Gamma_{ss}^\dagger}\right]^{-\mathbf{1}}\mathbf{b_t}} \tag{6}$$

2.3. Correlation Coefficients of the Voltages

When the dipole array is used for reception, the open circuit voltages $\mathbf{V}_{antO}$ induced from an impinging plane EM wave relate to the voltages $\mathbf{V}_{ant}$ propagated to the receiver front-end

$$\mathbf{V}_{ant} = \mathbf{Z}_{ss}(\mathbf{Z}_{tt} + \mathbf{Z}_{ss})^{-1}\mathbf{V}_{antO} \tag{7}$$

where $\mathbf{Z}_{ss}$ is the impedance matrix of the receiver multiport loads.

An important limiting factor to the array diversity performance is the magnitude of the covariance matrix elements of the induced voltages $\langle \mathbf{V}_{ant}\mathbf{V}_{ant}^* \rangle$ across the receiver-end loads which can be related to the open circuit voltages covariance matrix $\langle \mathbf{V}_{ant0}\mathbf{V}_{ant0}^* \rangle$, using Equation (7), as follows

$$\langle \mathbf{V}_{ant}\mathbf{V}_{ant}^* \rangle = \mathbf{Z}_{ss}(\mathbf{Z}_{tt} + \mathbf{Z}_{ss})^{-1} \langle \mathbf{V}_{ant0}\mathbf{V}_{ant0}^* \rangle (\mathbf{Z}_{tt} + \mathbf{Z}_{ss})^{-1\dagger}\mathbf{Z}_{ss}^\dagger \tag{8}$$

If two-dimensional fading Rayleigh channels are assumed, the covariance of the open circuit voltages $\langle v_{antOi}\overline{v_{antOi}} \rangle$ is analogous to the covariance $\langle |E_z| \rangle$ of the linear polarized and z-directed electric fields E_z for the zenith angle of incidence $\theta_0 = \pi/2$ at the dipoles centers, analogous to the effective heights H_{effi} and H_{effj} of the respective radiators [12], as

$$\langle v_{antOi}\overline{v_{antOi}} \rangle = \left\langle |E_z|^2 \right\rangle H_{effi}H_{effj}^* J_0(kd_{ij}) \tag{9}$$

where J_0 is the Bessel function of the first kind and zero order and d_{ij} is the distance between the radiators. The correlation values r_{ij} can be computed from the respective covariances $\langle v_{antOi}\overline{v_{antOj}} \rangle$ and the effect of the receiver can be incorporated into computations using (8), as

$$r_{ij} = \frac{\langle v_{antOi}\overline{v_{antOj}} \rangle}{\sqrt{\langle |v_{antOi}| \rangle^2 \langle |v_{antOj}| \rangle^2}} \tag{10}$$

2.4. Aperture Efficiency

A significant performance criterion of an antenna array is its effective aperture A_{eff} that depends on the intercepted power from incident electromagnetic waves arriving from the direction of its maximal gain, as follows

$$A_{eff} = \frac{\lambda^2}{4\pi} G \tag{11}$$

The aperture efficiency of an antenna array quantifies the received power, in respect to the total antenna area, as the ratio of its effective area A_{eff} to its physical area A_{phys}. Namely,

$$\epsilon_{aperture} = \frac{A_{eff}}{A_{phys}} \tag{12}$$

2.5. Particle Swarm Optimization

Particle Swarm Optimization exploits a set of potential solutions to the optimization problem called the swarm [1]. Each particle in the swarm represents a candidate solution scored by a fitness function, and its position in the multi-dimensional problem space is updated,

$$\begin{aligned} \upsilon_{k+1} &= \upsilon_k + c_1\rho_1(p_l - x_k) + c_2\rho_2(p_g - x_k) \\ \upsilon_{k+1} &= \text{sign}(\upsilon_{\text{k+1}}) \min(|\upsilon_{\text{k+1}}|, \upsilon_{\text{max}}) \\ x_{k+1} &= x_k + \upsilon_{k+1} \end{aligned} \tag{13}$$

where k denotes the generation number, x_k and υ_k the particle's position and velocity, and ρ_1, ρ_2 are random numbers between 0 and 1. The velocity update rule exploits the best position found by each particle x_l and the global best position x_g discovered so far by its neighbors. The individuality c_1 associates the particle's own experience with its current position, while the sociality c_2 defines the level of interaction between the particles of the same neighborhood. The velocity clamping υ_{max} constrains the particles velocity.

The Multi-Objective PSO algorithm stores a set of non-dominated solutions in an external archive, ranked using the Pareto optimality concept [6]. A solution is considered as Pareto optimal, if it minimizes at least one objective without making any other objective worse, compared to archived solutions. The algorithm does not implicitly exclude non-feasible solutions from the archive; it prioritizes archiving of feasible solutions over the non-feasible ones, taking also under consideration the respective violation of constraints. In this work, the speed-constrained SMPSO algorithm is used, that employs an appropriate constriction coefficient to limit the particles velocity [18]. The exploratory ability of the algorithm is enhanced by allowing each

particle to mutate with probability p_m using a polynomial probability distribution controlled by a positive index parameter η_m [19].

3. THE OPTIMIZED PHASED ARRAY

The spatial configuration of a symmetrical non-uniform linear phased array is optimized, constituted by 16 vertical half-wave dipoles with 0.0005λ wire radius. The candidate structures are represented by a solution vector $\mathbf{x}$, that encodes the relative placement of the array elements (Fig. 2). During the optimization, the MOPSO algorithm is allowed to place the dipoles up to a maximum distance of one wavelength apart. In order to evaluate the radiation pattern and the mutual coupling of the candidate designs, the dipoles are partitioned into 15 segments and triangular basis functions are used to approximate the current distribution resulted by the MoM analysis.

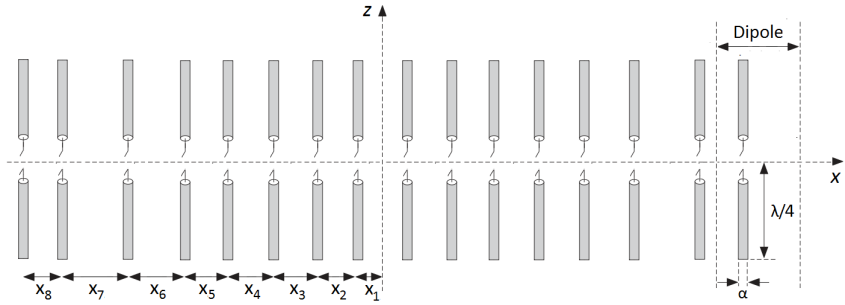

Figure 2. Symmetrical non-uniform linear array of $\lambda/2$ dipoles.

Two fitness functions are defined; $f_{sidelobe}$ evaluates the achieved reduction in sidelobe level SL and $f_{correlation}$ evaluates the maximum correlation factor r_{ij} between radiators. The functions are separately evaluated over the obtained pattern for the maximum scan angle θ_0 and are subject to computed conjugate matching at broadside, respectively, as

$$\begin{aligned} f_{sidelobe} &= SL_{\theta_0} \\ f_{correlation} &= \max\left[r_{ij}\right]_{i\neq j} \end{aligned} \tag{14}$$

Enforced constraints dictate that the aperture efficiency of the candidate arrays should exceed the efficiency of a uniform linear array (ULA) with inter-element spacing of $d_0 = 0.5\lambda$, the maximum r_{ij} from the computed correlation matrix should not exceed a value of 0.6 and finally the overall matching factor $q(\theta)$ should maintain a value of 0.5

or better over the scan angles range 0° to θ_0. Therefore,

$$\begin{aligned} g_{aperture} &= \epsilon_{aperture} - \epsilon_{aperture,d_0=\lambda/2} \geq 0 \\ g_{correlation} &= \max\left[r_{i,j}\right]_{i\neq j} \leq 0.6 \\ g_{matching} &= \min\left[q(\theta)\right]_{\theta=0}^{\theta_0} \geq 0.5 \end{aligned} \tag{15}$$

4. NUMERICAL RESULTS

4.1. Optimized Spatial Array Configurations

The optimization parameters used are those suggested by Nebro et al. in [18]; individuality c_1 and sociality c_2 were allowed to take values in the range 1.5 to 2.5, while the archive and swarm population size were set equal to 50. The mutation probability p_m was chosen as the inverse of the problem dimensionality and a distribution index value η_m of 60 was set to enhance the algorithm's search capabilities. In an effort to approximate the true Pareto set of the problem, the optimization was repeated 10 times and results were combined in a single front populated by 50 solutions (Fig. 3). The algorithm was allowed to evolve for 200 generations and 45 solutions were obtained on average from each run.

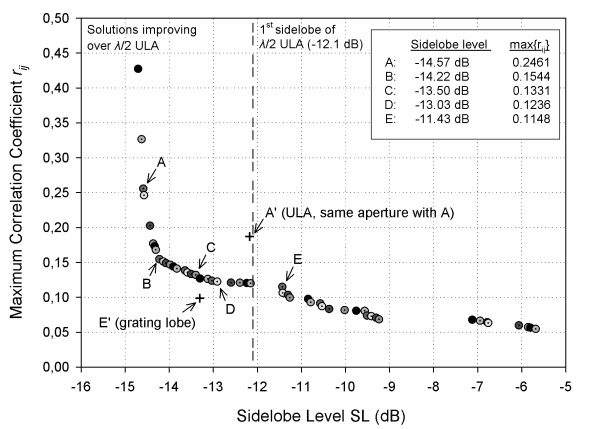

Figure 3. Pareto set characteristic of the trade-off between array correlation and sidelobes level, when diagram is steered 60°.

Each non-dominated solution represents a different array configuration and can be interpreted as an optimal design; any other perturbation of the dipoles position that may result in the same maximum correlation coefficient value, can not feature lower sidelobes. Obtained arrays can be grouped into those that feature lower sidelobes

than a uninform $\lambda/2$ spaced dipole array and those with higher sidelobes. This is reflected in Fig. 3, where 26 solutions are shown to improve over the ULA case. This solution subset represents designs that span a range of maximum correlation values of 0.12 to 0.43 and maximum sidelobe level of -12.2 to -14.7 dB. Four different spatial configurations were sampled from the prescribed range and one from the complementary solution space; these are summarized in Table 1.

In Fig. 4, the normalized gain diagram of the candidate array A is compared to the radiation diagram of a ULA A' with the same aperture. The non-uniform array A reduces the peak sidelobe level by 2.4 dB compared to A', and both arrays have approximately the same beamwidth, due to the fixed aperture of 6.58λ. If the algorithm was allowed to position more closely the dipoles, further suppression of sidelobes would be possible, at the expense of diversity performance.

The maximum steerability of a uniform linear phased array with d_0 elements spacing is $\theta_0 = \sin^{-1}(\lambda/d_0 - 1)$. A ULA E' with the same widened aperture of 9.4λ to optimized array E, has a predicted maximum steerability of 36.6°. Consequently, the equivalent design E'

Table 1. Radiator positioning (in λ) of the selected arrays.

	$\mathbf{d_1}$	$\mathbf{d_2}$	$\mathbf{d_3}$	$\mathbf{d_4}$	$\mathbf{d_5}$	$\mathbf{d_6}$	$\mathbf{d_7}$	$\mathbf{d_8}$	$\max\{\mathbf{r_{ij}}\}$
A	0.225	0.618	1.011	1.433	1.822	2.346	2.939	3.291	0.2461
B	0.213	0.667	1.14	1.574	2.034	2.591	3.167	3.525	0.1544
C	0.239	0.695	1.173	1.644	2.179	2.545	3.126	3.63	0.1331
D	0.248	0.724	1.225	1.716	2.227	2.624	3.195	3.719	0.1236
E	0.248	1.242	1.755	2.232	3.164	3.692	4.208	4.701	0.1158

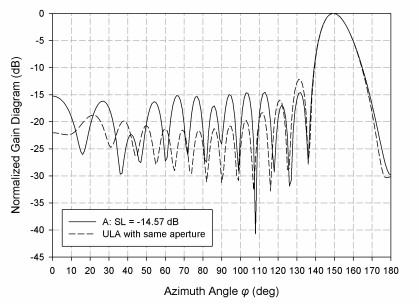

Figure 4. Normalized gain diagram of array configurations A and A'.

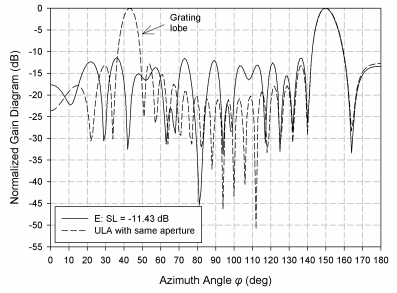

Figure 5. Normalized gain diagram of array configurations E and E'.

is presented as an outlier to solutions enclosed by the Pareto front and its position in Fig. 3 is determined by the level of its first sidelobe.

The steered at 60° from broadside radiation pattern of the ULA E' is shadowed by a grating lobe in contrast to the non-uniform array E with a sidelobe suppression of 11.43 dB as shown in Fig. 5. Both arrays feature the same beamwidth since their aperture is equal. It can be concluded that the obtained non-uniform arrays, having apertures bigger than the uninform $\lambda/2$-spaced dipole array case, present similar radiation characteristics to thinned aperiodic linear arrays [9].

Arrays were optimized at the maximum specified scan angle, in order to secure that their performance is maintained, while the main beam is steered at intermediate angles. Additional simulations were conducted to assess the sidelobes variation during scanning and the results are presented in Fig. 6. All designs, except from the thinned array E, outperform a ULA with element spacing of 0.5λ. Arrays A and B exhibit almost equal suppression of sidelobes at broadside and maximum scan angle, while solutions C and D have better performance at broadside. The variations can be attributed to the enforced array symmetry; nevertheless this is an essential condition if the main beam of the array should be steered equally well at both directions.

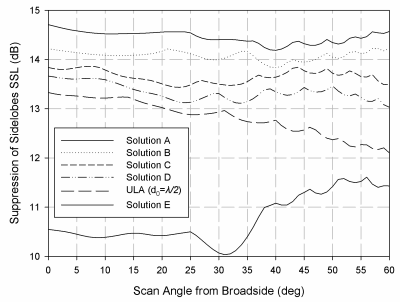

Figure 6. Suppression of sidelobes for the selected configurations.

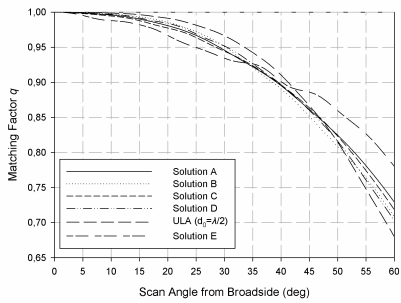

Figure 7. Overall mismatch of the selected array configurations.

Finally, the performance of the matching sections is evaluated by the matching factor q, while the candidate arrays are scanned away from broadside, and the results are summarized in Fig. 7.

Overly, the results for the selected solutions confirm that none of the optimized array configurations violates the condition of 0.5 minimum matching efficiency. It also can be observed that the ULA exhibits a greater degree of mismatching in large scan angles than the non-uniform arrays obtained by the optimization runs.

4.2. Sensitivity Analysis for Phase Variations

Contemporary phased-array systems are designed to use digital phase shifters that feature a finite granularity, depending on the number of quantatization bits employed to encode phase information. Additional phase error is introduced by non-linearities of phase shifters, and by the use of time-delaying networks (i.e., in corporate feed networks), that may further impact the array radiation characteristics. In this work, sensitivity analysis of the obtained solutions is carried out for varying maximal phase error of $1\%, 2\%, \ldots, 5\%$ introduced to the incident at array ports voltage waves $\mathbf{a_t}$, as an additional design criterion. Monte-Carlo simulation results of selected low sidelobe solutions, for the 5% error scenario and 200 samples, are depicted in Fig. 8.

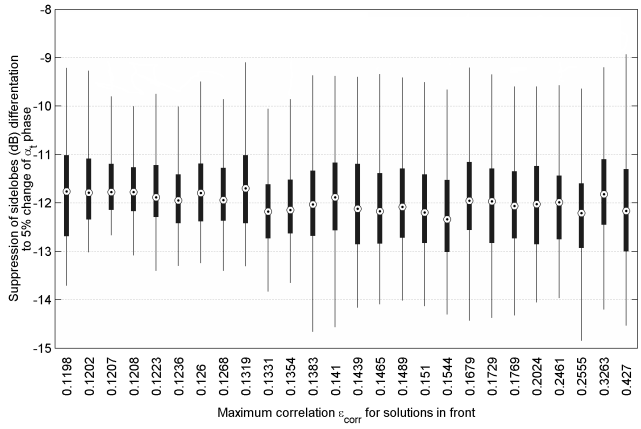

Figure 8. Sensitivity analysis of solutions for 5% phase error.

The computed variations in sidelobe level were found to follow normal distributions, their depicted extent is representative of the 25th and 75th percentiles, and marked points are the respective median values. Some candidate array solutions were less susceptible to feed phase errors than others, rendering them more fit to be used in system implementations where larger errors are expected.

In the interest of establishing a performance envelop on candidate solutions, a parametric exponential curve was modeled that approximates the distribution of the median SL points against the maximum ϵ_{corr} correlation values, for different error scenarios, as

$$SL_{median}(i) = \alpha + be^{-k\epsilon_{corr}(i)} \tag{16}$$

The interpolating parameters α, b and k computed from Monte-Carlo simulations for the defined phase error margin of 1%–5%, along

Table 2. Interpolation parameters for different phase error scenarios.

	1%	**2%**	**3%**	**4%**	**5%**	**Mean Difference**
α	−14.507	−14.007	−13.479	−12.958	−12.365	0.535
b	33.823	35.731	38.413	39.879	41.752	1.982
k	24.027	25.751	27.803	29.361	31.267	1.81
$RMSE$	0.432	0.418	0.392	0.393	0.392	-

Table 3. Predicted vs. computed interpolation parameters from 10% phase error simulations data.

	α	b	k	$RMSE$
predicted	−9.688	51.663	40.316	0.396
computed	−9.726	38.289	36.077	0.379
difference	0.39%	34.9%	11.8%	4.6%

with Root Mean-Square Error values, are summarized in Table 2.

It is possible to develop a predictor based on the mean differences of the fitting curve parameters, as computed from the simulation data,

$$\hat{p}(e) = p(1) + (e-1)\frac{1}{N-1}\sum_{n=1}^{N-1}(p(n+1) - p(n)) \qquad (17)$$

where index n corresponds to the different error values of the $N = 5$ consequent runs and $\hat{p}(e)$ is the expected value for one of the interpolation parameters α, b or k, for phase error e%. In order to assess the accuracy of the above formulation, the predicted parameters are compared to the computed interpolation parameters from a 10% phase error simulation, and the results are presented in Table 3.

In Fig. 9 are shown the median sidelobe curves computed for phase errors of 1%–5%, the curve predicted for a 10% phase error scenario and the respective sidelobes median values. The presented results indicate that the obtained prediction does not deviate significantly from simulation results, in terms of root mean square error. This approximation is very useful for outlining a performance envelop for the candidate linear arrays, subject to the correlation coefficient constraints already discussed, without needing to resort

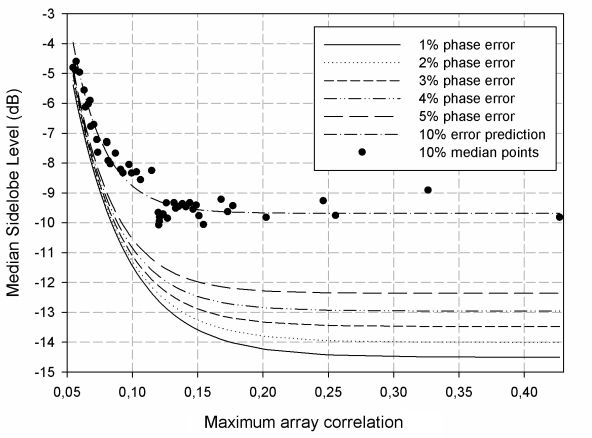

Figure 9. Median SL curves computed for phase errors of 1%–5%, prediction curve for 10% phase error and respective SL median values.

to computationally intensive Monte-Carlo simulations. Performance envelopes established herein indicate that the optimized arrays radiation characteristics are tolerant to feed phase variations expected in realistic implementations ($\leq \pm 5\%$).

5. CONCLUSIONS

The paper has presented a novel methodology for optimizing the spatial configuration of linear phased arrays, in terms of minimizing the voltage correlation at the receiver front-end and the sidelobe level when the main beam is steered to a maximum specified scan angle. Restrictions were enforced on one hand on the maximum allowed mismatch during array scanning in order to minimize the power reflected back to the source network, and on the other hand on the aperture efficiency to retain comparable gain to uniform linear arrays with comparable apertures. To the best of the authors' knowledge, this is the first study that combines optimization goals related to radiation pattern synthesis and diversity performance of an antenna array. After optimizing a $\lambda/2$ dipole symmetric linear array and assuming a two-dimensional Rayleigh channels electromagnetic environment, the obtained results indicate that there is a trade-off between the distance among radiators and the desired correlation values. The radiation characteristics of the optimized array configurations were shown to be tolerant to feed phase variations that appear in realistic implementations.

REFERENCES

1. Kennedy, J., "Swarm intelligence," *Handbook of Nature-Inspired and Innovative Computing*, 187–219, Springer, 2006.
2. Li, W. T., X. W. Shi, and Y. Q. Hei, "An improved particle swarm optimization algorithm for pattern synthesis of phased arrays," *Progress In Electromagnetics Research*, Vol. 82, 319–332, 2008.
3. Donelli, M., R. Azaro, F. G. B. De Natale, and A. Massa, "An innovative computational approach based on a particle swarm strategy for adaptive phased arrays control," *IEEE Trans. Antennas Propagat.*, Vol. 54, No. 3, 888–898, 2006.
4. Boeringer, D. W. and D. H. Werner, "Efficiency-constrained particle swarm optimization of a modified bernstein polynomial for conformal array excitation amplitude synthesis," *IEEE Trans. Antennas Propagat.*, Vol. 53, No. 8, 2662–2673, 2005.
5. Jin, N. B. and Y. Rahmat-Samii, "Parallel particle swarm optimization and finite-difference time-domain (PSO/FDTD) algorithm for multiband and wide-band patch antenna designs," *IEEE Trans. Antennas Propagat.*, Vol. 53, No. 11, 3459–3468, 2005.
6. Coello, C. A. C., G. T. Pulido, and M. S. Lechuga, "Handling multiple objectives with particle swarm optimization," *IEEE Trans. Evolutionary Comput.*, Vol. 8, No. 3, 256–279, 2004.
7. Jin, N. and Y. Rahmat-Samii, "Advances in particle swarm optimization for antenna designs: Real-number, binary, single-objective and multiobjective implementations," *IEEE Trans. Antennas Propagat.*, Vol. 55, No. 3, 556–567, 2007.
8. Chamaani, S., M. S. Abrishamian, and S. A. Mirtaheri, "Multi-objective optimization of UWB monopole antenna," *Progress In Electromagnetics Research C*, Vol. 8, 83–94, 2009.
9. Bray, M. G., D. H. Werner, D. W. Boeringer, and D. W. Machuga, "Optimization of thinned aperiodic linear phased arrays using genetic algorithms to reduce grating lobes during scanning," *IEEE Trans. Antennas Propagat.*, Vol. 50, No. 11, 1732–1742, 2003.
10. Zhu, Y. Z., Y. J. Xie, Z. Y. Lei, and T. Dang, "A novel method of mutual coupling matching for array antenna design," *Journal of Electromagnetic Waves and Applications*, Vol. 21, No. 8, 1013–1024, 2007.
11. Wallace, J. W. and M. A. Jensen, "Termination-dependent diversity performance of coupled antennas: Network theory analysis," *IEEE Trans. Antennas Propagat.*, Vol. 52, No. 1, 98–105, 2004.

12. Broydé, F. and E. Clavelier, "Taking advantage of mutual coupling in radio-communication systems using a multi-port antenna array," *IEEE Antennas Propag. Mag.*, Vol. 49, No. 4, 208–220, 2007.
13. Harrington, R. F., *Field Computation by Moment Methods*, Wiley-IEEE Press, 1993.
14. Orfanidis, S. J., *Electromagnetic Waves and Antennas*, Rutgers University, 2004.
15. Takamizawa, K., "Analysis of highly coupled wideband antenna arrays using scattering parameter network models," 45–60, the Faculty of the Virginia Polytechnic Institute and State University, Virginia, 2002.
16. Pozar, D. M., *Microwave Engineering*, Wiley-India, 2009.
17. Weber, J., C. Volmer, K. Blau, R. Stephan, and M. A. Hein, "Miniaturized antenna arrays using decoupling networks with realistic elements," *IEEE Trans. Microwave Theory and Tech.*, Vol. 54, No. 6, 2733–2740, 2006.
18. Nebro, A. J., J. J. Durillo, J. García-Nieto, C. A. C. Coello, F. Luna, and E. Alba, "SMPSO: A new PSO metaheuristic for multi-objective optimization," *Proc. 2009 IEEE Symposium on Computational Intelligence in Multi-criteria Decision-making*, 66–73, Mar. 30–Apr. 2, 2009.
19. Deb, K., *Multi-Objective Optimization Using Evolutionary Algorithms*, John Wiley & Sons, 2001.